High quality above 3-μm mid-infrared InGaAsSb/AlGaInAsSb multiple-quantum well grown by molecular beam epitaxy*

Xing Jun-Liang(邢军亮), Zhang Yu(张 宇), Xu Ying-Qiang(徐应强), Wang Guo-Wei(王国伟), Wang Juan(王 娟), Xiang Wei(向 伟), Ni Hai-Qiao(倪海桥), Ren Zheng-Wei(任正伟), He Zhen-Hong(贺振宏), and Niu Zhi-Chuan(牛智川)†

State Key Laboratory for Superlattices and Microstructures, Institute of Semiconductors, Chinese Academy of Sciences, Beijing 100083, *China*

(Received 25 April 2013; revised manuscript received 10 May 2013; published 3 December 2013)

The GaSb-based laser shows its superiority in the 3–4 μm wavelength range. However, for a quantum well (QW) laser structure of InGaAsSb/AlGaInAsSb multiple-quantum well (MQW) grown on GaSb, uniform content and high compressive strain in InGaAsSb/AlGaInAsSb are not easy to control. In this paper, the influences of the growth temperature and compressive strain on the photoluminescence (PL) property of a 3.0-μm InGaAsSb/AlGaInAsSb MQW sample are analyzed to optimize the growth parameters. Comparisons among the PL spectra of the samples indicate that the $In_{0.485}GaAs_{0.184}Sb/Al_{0.3}Ga_{0.45}In_{0.25}As_{0.22}Sb_{0.78}$ MQW with 1.72% compressive strain grown at 460 °C posseses the optimum optical property. Moreover, the wavelength range of the MQW structure is extended to 3.83 μm by optimizing the parameters.

Keywords: GaSb, multiple-quantum well, photoluminescence

PACS: 78.55.Cr, 78.66.Fd, 78.67.De **DOI:** 10.1088/1674-1056/23/1/017805

1. Introduction

The GaSb-based alloy, which shows its superiority in the 3–4 μm wavelength range, has attracted a great deal of attention due to its application in the mid-infrared optoelectronic devices during the last decade. The antimonide strain quantum well (QW) laser diode is an appealing candidate for applications including gas analysis, free space communication and countermeasure. The laser diodes operating in a continuous-wave (CW) mode at room temperature in the spectral region of 2–3 μm have been fabricated.[1–5] Type-I InGaAsSb/ AlGaAsSb strained QW lasers operating at room temperature (RT) within the spectral region of 2.3–2.7 μm provide output powers of hundreds of mW in the CW mode.[6,7] However, the increasing indium content in the QWs to extend the emission wavelength above 3 μm results in a strong reduction of the valance band offset and a rapid degradation of the optical performance.[8] In order to solve this problem, a quinternary AlGaInAsSb barrier material was utilized and a heavy compressive strain above 1% was introduced. RT CW output powers of 190 mW, 165 mW, and 50 mW for devices emitting at 3.1 μm, 3.2 μm, and 3.3 μm were demonstrated, respectively, and RT CW operation up to 3.73 μm was achieved.[9–11] The optical quality is still not good due to the difficulty in precisely controlling the contents and the strains of the InGaAsSb QW materials. Therefore, it becomes an extremely important issue to optimize the growth parameters for obtaining high optical quality QWs with long wavelength above 3 μm.

In this paper, we conduct a detailed study of the effects of the growth temperature and compressive strain on the photoluminescence (PL) properties of 3.0 μm multiple-quantum-well (MQW) samples grown by molecular beam epitaxy (MBE). The dependences of the PL spectra of various MQW samples on the compressive strain and growth temperature are measured and analyzed to optimize these parameters. Moreover, the wavelength range of the MQW structure is extended to 3.83 μm by optimizing the parameters. This result indicates that it is promising to fabricate the 3–4 μm laser diodes based on InGaAsSb/AlGaInAsSb strained QWs.

2. Experiment

All MQW samples investigated in this paper were fabricated on Te-doped (001) oriented GaSb substrates using a VG80 solid-source MBE system, which was equipped with As and Sb valved crackers. *In-situ* reflection high-energy electron diffraction (RHEED) was used to characterize the surface and monitor the epitaxial growth. The growth temperature was calibrated to the GaSb restructure ($2 \times 5 \rightarrow 1 \times 3$) temperature at a pyrometer reading of 495 °C in our system. After a 300-nm GaSb buffer layer was grown at 600 °C, the substrate temperature was lowered to the growth temperature. Three 10-nm $In_{0.485}GaAs_xSb$/20-nm $Al_{0.3}Ga_{0.45}In_{0.25}As_{0.22}Sb_{0.78}$ QWs were grown under a V/III pressure ratio of 15, including the

*Project supported by the National Basic Research Program of China (Grant Nos. 2013CB932904, 2012CB932701, 2011CB922201, and 2010CB327600), the National Special Funds for the Development of Major Research Equipment and Instruments, China (Grant No. 2012YQ140005), and the National Natural Science Foundation of China (Grant Nos. 61274013, U1037602, and 61290303).

†Corresponding author. E-mail: zcniu@semi.ac.cn

© 2014 Chinese Physical Society and IOP Publishing Ltd

growth interruption at the interface. A schematic diagram of the basic layer structure is shown in Fig. 1. In order to analyze the influence of the growth parameters on the PL spectra of GaSb-based MQW structures, two sets of samples with different growth temperatures and compressive strains were fabricated. Samples A1–A5 comprised of $In_{0.485}GaAs_{0.201}Sb$ MQWs with compressive strain 1.61% were grown at 500 °C, 480 °C, 460 °C, 440 °C, and 420 °C, respectively. The compressive strains in the MQWs of the other series, which were grown at 460 °C, varied. The strains in samples B1–B4 were 1.28%, 1.61%, 1.72%, and 1.84%, respectively.

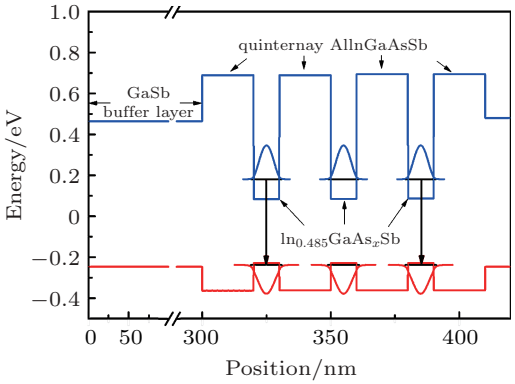


Fig. 1. (color online) Layer structure of the InGaAsSb/AlGaInAsSb MQW.

Atomic force microscopy (AFM) and high-resolution X-ray diffraction (HRXRD) measurements were carried out to analyze the surface morphologies and structural characteristics of the as-grown samples. The optical property was investigated by using room temperature PL spectra. The PL signal was excited by a 628-nm semiconductor laser, spectrally dispersed through a Fourier transform infrared spectrometer, and detected by a liquid-nitrogen-cooled HgCdTe detector.

3. Optimization of 3.0 μm quantum well

3.1. Growth temperature-dependent samples

Figure 2(a) shows the dependences of the PL spectra of the $In_{0.485}GaAs_{0.201}Sb/Al_{0.3}Ga_{0.45}In_{0.25}As_{0.22}Sb_{0.78}$ MQW samples at 300 K on the growth temperature, indicating the radioactive recombination processes in these MQW structures. The dominant strong peak at 0.413 eV is due to the transition between the first heavy hole level (1hh) and the first electron level (1e). The weak discrepancy in the PL peaks of the QWs is attributed to alloy content fluctuation and gradations in the QWs. The shoulders at the high energies are ascribed to the In-content segregation.[12] The peak labeled as substrate peak at 0.758 eV in Fig. 2(a) originates from a donor–acceptor transition in the bulk GaSb.[13] The splitting of the main PL peak is present from 0.471 eV to 0.496 eV, which may be explained by taking into account the strongest water vapor absorption lines at 2.605 μm, 2.596 μm, and 2.594 μm. The integrated PL intensity and the full width at half maximum (FWHM) of the QW peak are analyzed to characterize the optical properties. Figure 2(b) demonstrates the trends each as a function of the growth temperature. The integrated PL intensity is continuously enhanced with decreasing growth temperature and saturated at the optimum temperature of 460 °C (sample A3). This is attributed to the improvement in the abruptness of the interface, which results from the reduced surface migration of III group element with the decrease of temperature.[14–16] Below 460 °C, the integrated PL intensity decreases, as the crystalline quality of the InGaAsSb layer is likely to be deleteriously affected at lower growth temperature. A higher density of non-irradiative recombination centers may be generated due to the reduction of the In atom segregation.

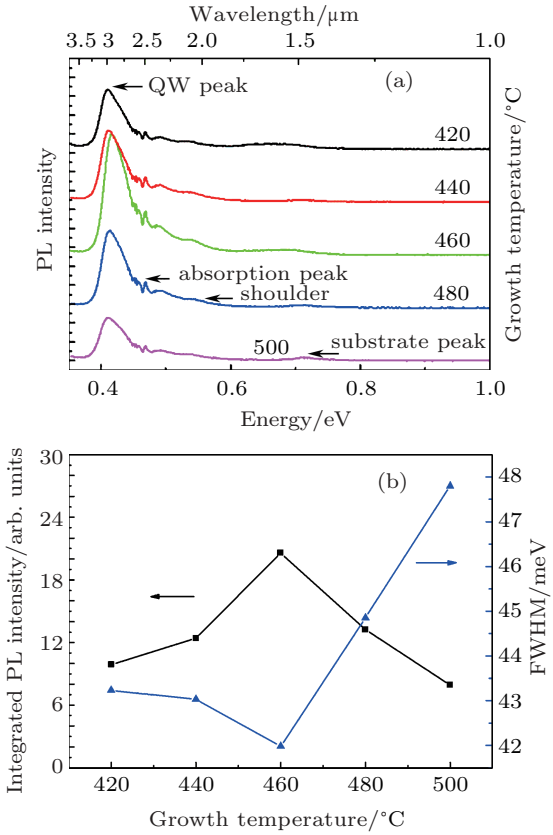


Fig. 2. (color online) (a) The PL spectra of the 10-nm $In_{0.485}GaAs_{0.201}Sb/Al_{0.3}Ga_{0.45}In_{0.25}As_{0.22}Sb_{0.78}$ MQW samples at 300 K versus the growth temperature in series A. (b) Integrated PL intensity and FWHM of the $In_{0.485}GaAs_{0.201}Sb/Al_{0.3}Ga_{0.45}In_{0.25}As_{0.22}Sb_{0.78}$ MQW samples versus the growth temperature. The FWHMs of the samples are indicated by the solid triangles.

This is consistent with the FWHM trends in Fig. 2(b). The optimum linewidth, 41.9 meV, is also achieved by sample A3 grown at 460 °C. The significant decrease of the FWHM in sample A3 can well be explained by an improved surface and extremely abrupt interfaces. HRXRD rocking curves and an AFM image from sample A3 are shown in Fig. 3. The root mean square (RMS) roughness of sample A3 is 0.477 nm in a 10 μm×10 μm scan area, which is the minimum in series A samples. Besides, the satellite peaks in the HRXRD rocking

curves of sample A3 with highly strained layers are also a sign of perfect interface quality. Reducing the growth temperature suppresses the surface segregation and interdiffusion of group III, which effectively prevents the atomic composition of the MQW structure from gradually changing from an abrupt interface to a graded profile.[17] This induces a reinforcement of the confinement for holes and electrons in the QWs to improve the performances.

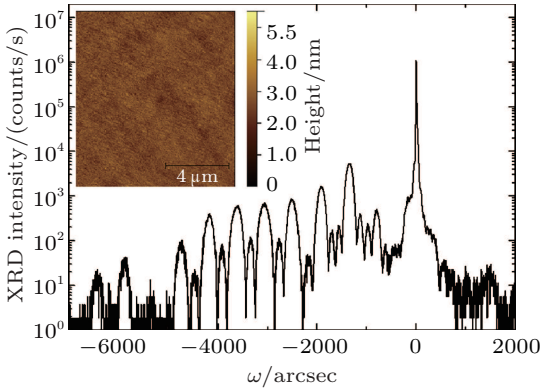


Fig. 3. (color online) Experimental HRXRD rocking curve of sample A3 grown at 460 °C and an AFM image (10 μm×10 μm) on sample A3 (inset).

3.2. Strain-dependent samples

Figure 4(a) shows the dependences of the room temperature PL spectra of series B samples on the compressive strain in QWs. The strain in MQW can be controlled by the As content in well material $In_{0.485}GaAs_xSb$. The strain can be found by fitting with HRXRD. The experimental HRXRD rocking curve of sample B2 is in good agreement with the simulated rocking curve, which is shown in Fig. 4(b). As shown in the fitting result, the compressive strain of sample B2 is 1.61%. The same fitting is carried out for all samples in series B, and the compressive strains in samples B1–B4 are 1.27%, 1.61%, 1.72%, and 1.84%, respectively. The PL spectra of the $In_{0.485}GaAs_xSb/Al_{0.3}Ga_{0.45}In_{0.25}As_{0.22}Sb_{0.78}$ MQW samples exhibit very similar features to those in Fig. 2(a); besides, the QW peak indicated by the arrow is blue-shifted in PL energy from 0.409 eV to 0.424 eV as the compressive strain in the QWs increases from 1.27% to 1.84%. The observed blueshift of the QW peak can be well explained by the fact that the 1e band rises faster than the 1hh band with the compressed strain in the sample increased.

The integrated PL intensity and the FWHM of the MQW samples in series B are shown in Fig. 5(a). With increasing compressive strain in the QWs, the FWHM of the MQW peak continuously decreases. This is well explained as the position of the heavy hole band raised by the compressive strain in the QWs.[18] Figure 5(b) shows the calculated valence band offset between $In_{0.485}GaAs_xSb$ and quinternary $Al_{0.3}Ga_{0.45}In_{0.25}As_{0.22}Sb_{0.78}$ (based on Refs. [19] and [20]),

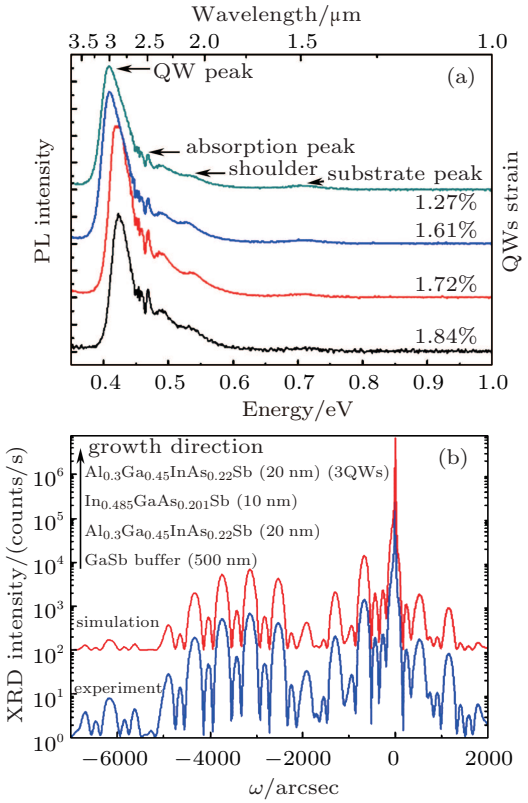


Fig. 4. (color online) (a) The PL spectra of the 10-nm $In_{0.485}GaAs_xSb/Al_{0.3}Ga_{0.45}In_{0.25}As_{0.22}Sb_{0.78}$ MQW samples at 300 K versus the compressive strain in series B. (b) Experimental and simulated HRXRD rocking curves of sample B2, the simulation rocking curve is for an MQW structure consisting of three wells and four barriers with 1.61% compressive strain.

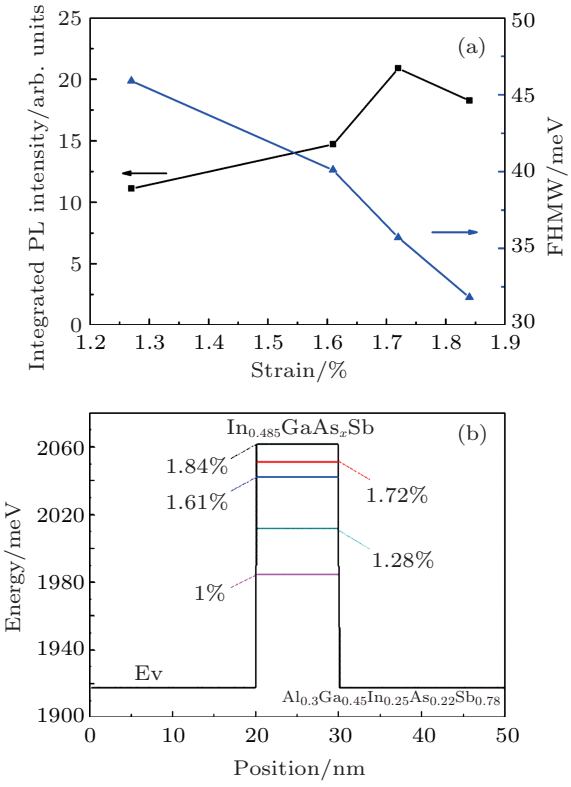


Fig. 5. (color online) (a) Integrated PL intensity and FWHM of $In_{0.485}GaAs_xSb/Al_{0.3}Ga_{0.45}In_{0.25}As_{0.22}Sb_{0.78}$ MQW versus the compressive strain. The FWHM of the MQW peak is indicated by the solid triangle. (b) Calculated valence band offset versus solid angle position for different compressive strains.

which indicates that the more compressive the strain, the higher the heavy hole band. The deeper heavy hole band induces a greater band offset in the valance band, which means an improved hole confinement. Besides, the heavy strain can also suppress the Auger recombination process. Both effects improve the optical qualities of the QWs. Although the MQW samples with heavy strain have superior optical properties, the integrated intensity of the PL spectrum deteriorates when the compressive strain in the QWs is larger than the optimum value (1.72%). The heavier internal strain in the $In_{0.485}GaAs_xSb$ QWs may cause more dislocations which act as non-radioactive recombination centers.[21]

4. Above 3.0 μm quantum well

$InGaAsSb/Al_{0.3}Ga_{0.45}In_{0.25}As_{0.22}Sb_{0.78}$ MQW samples with the emission peaks ranging from 2.7 μm to 3.83 μm were fabricated by precisely controlling the In and As contents in InGaAsSb under the optimum parameters. The FWHMs of the QW peaks are 35.9 meV, 43.1 meV, 36.6 meV, 42.1 meV, and 47.3 meV, respectively, which are shown in Fig. 6(a). Figure 6(b) shows the dark-field image of the 3.83-μm MQW sample under a diffraction condition of $g = 002$, which is very sensitive to the content in the alloy. The contents are indicated in the figure. The good structural quality of the above 3 μm MQW inferred from HRXRD is directly confirmed by a cross-section TEM.

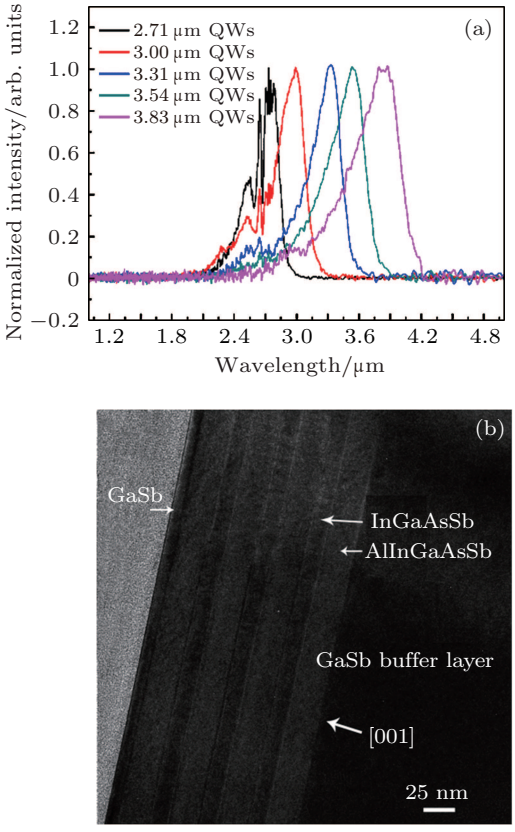


Fig. 6. (color online) (a) Normalized room temperature PL spectra of the 2.7–3.83 μm $InGaAsSb/Al_{0.3}Ga_{0.45}In_{0.25}As_{0.22}Sb_{0.78}$MQW samples grown with optimum growth parameters. (b) Dark-field TEM image of the 3.8-μm MQW sample grown on GaSb (001) along the [110] zone axis, which contains three QWs.

5. Conclusion

We grow InGaAsSb/AlGaInAsSb MQW structures with different compressive strains at various growth temperatures. Using HRXRD, AFM, and TEM, we investigate the surface morphologies and structural characteristics of the samples. The dependences of the PL integrated intensity and FWMH on the growth temperature and compressive strain indicate that the $In_{0.485}GaAs_{0.184}Sb/Al_{0.3}Ga_{0.45}In_{0.25}As_{0.22}Sb_{0.78}$ MQW with 1.72% compressive strain grown at 460 °C owns the optimum optical properties. Moreover, we extend the wavelength range of the MQW structure to 3.83 μm by optimizing the parameters.

References

[1] Lin C, Grau M, Dier O and Amann M C 2004 *Appl. Phys. Lett.* **84** 5088
[2] Donetsky D, Kipshidze G, Shterengas L, Hosoda T and Belenky G 2007 *Electron. Lett.* **43** 810
[3] Chen J F, Donetsky D, Shterengas L, Kisin M V, Kipshidze G and Belenky G 2008 *IEEE J. Quantum. Electon.* **44** 1204
[4] Gupta J A, Barrios P J, Lapointe J, Aers G C and Storey C 2009 *Appl. Phys. Lett.* **95** 041104
[5] Naehle L, Belahsene S, von Edlinger M, Fischer M, Boissier G, Grech P, Narcy G, Vicet A, Rouillard Y, Koeth J and Worschech L 2011 *Electron. Lett.* **47** 46
[6] Rattunde M, Schmitz J, Kaufel G, Kelemen M, Weber J and Wagner J 2006 *Appl. Phys. Lett.* **88** 081115
[7] Kashani-Shirazi K, Vizbaras K, Bachmann A, Arafin S and Amann M C 2012 *IEEE Photonic. Tech. Lett.* **21** 1106
[8] Belenky G, Shterengas L, Kipshidze G and Hosoda T 2011 *IEEE. J. Sel. Top. Quant.* **17** 1426
[9] Belenky G, Shterengas L, Wang D, Kipshidze G and Vorobjev L 2009 *Semicond. Sci. Tech.* **24** 115013
[10] Hosoda T, Kipshidze G, Tsvid G, Shterengas L and Belenky G 2010 *IEEE Photonic. Tech. Lett.* **22** 718
[11] Vizbaras K and Amann M C 2012 *Semicond. Sci. Technol.* **27** 032001
[12] Wu X H, Elsass C R, Abare A, Mack M, Keller S, Petroff P M, Den-Baars S P, Speck J S and Rosner S J 1998 *Appl. Phys. Lett.* **72** 692
[13] Dutta P S, Koteswara Rao K S R, Bhat H L and Kumar V 1995 *Appl. Phys. A* **61** 149
[14] Kaspi R and Evans K R 1995 *Appl. Phys. Lett.* **67** 819
[15] Nagle J, Landesman J P, Larive M, Mottet C and Bois P 1993 *J. Cryst. Growth* **127** 550
[16] Yuan Z L, Xu Z Y , Xu J Z, Zheng B Z, Luo C P, Yang X P and Zhang P H 1996 *Chin. Phys.* **4** 523
[17] Muraki K, Fukatsu S, Shiraki Y and Ito R 1992 *Appl. Phys. Lett.* **61** 557
[18] Motyka M, Sek G, Ryczko K, Misiewicz J, Belahsene S, Boissier G and Rouillard Y 2009 *J. Appl. Phys.* **106** 066104
[19] Vurgaftman I, Meyer J R and Ram-Mohan L R 2001 *J. Appl. Phys.* **89** 5815
[20] Donati G P, Kaspi R and Malloy K J 2003 *J. Appl. Phys.* **94** 5814
[21] Gu Y, Zhang Y G, Song Y X, Ye H , Cao Y Y, Li A Z and Wang S M 2013 *Chin. Phys. B* **22** 37802